ResearchGate

See discussions, stats, and author profiles for this publication at: https://www.researchgate.net/publication/231434348

Ab initio calculations on vibronic coupling in the lower triplet states of pyrimidine

ARTICLE *in* CHEMINFORM · NOVEMBER 1992

Impact Factor: 0.74 · DOI: 10.1021/ja00050a038

CITATIONS
9

READS
18

3 AUTHORS, INCLUDING:

Wybren J Buma
University of Amsterdam
184 PUBLICATIONS **2,459** CITATIONS

SEE PROFILE

Available from: Wybren J Buma
Retrieved on: 02 February 2016

systems where the ground state of the π cation radical has been experimentally determined. The method was then used to determine the effect of substituents in cases where the ground state is unknown. Meso substituents that are electron donating lead to a $^2A_{2u}$ ground state, while those that are electron withdrawing lead to a $^2A_{1u}$ ground state. The β-substituted porphyrins maintained the $^2A_{1u}$ π cation radical ground state of the unsubstituted porphine and have a smaller effect on the relative energies of the $^2A_{1u}$ and $^2A_{2u}$ states compared to the meso substituents. Multivariate linear regression analyses, reflecting basic electronic principals, indicate that a balance between π effects, which tend to destabilize the a_{2u} and a_{1u} orbitals, and σ effects, which generally stabilize the orbitals, can explain the state energy orderings of the substituted Mg(II) porphyrins studied here. These states can be distinguished by experimental techniques such as NMR, EPR, and ENDOR that monitor the extent of unpaired spin on the substituents and porphyrin ring atoms. Since protoporphyin IX, the most commonly occurring porphyrin group in endogenous heme proteins, does not have meso substituents but has only β substituents, as do all the other naturally occurring porphyrins found in heme proteins, it would be expected to form $^2A_{1u}$ π cation states in the four-coordinate Mg(II) case. However, substitution of Fe for Mg and addition of axial ligands can be further modulators of these states and can lead to different ground states and properties. Future studies will address the role of these additional factors in determining the nature and selective stability of their π cation states.

Acknowledgment. We would like to thank Drs. Ping Du and Jack Fajer for helpful discussions during the course of this study. Support from the National Science Foundation (Grant No. DMB-9096181) for this work is gratefully acknowledged.

Ab-Initio Calculations on Vibronic Coupling in the Lower Triplet States of Pyrimidine

W. J. Buma,*,† M. C. J. M. Donckers,‡ and E. J. J. Groenen*,‡

Contribution from the Chemistry Department, University of California, Riverside, California 92521, and Center for the Study of Excited States of Molecules, Huygens Laboratory, University of Leiden, P.O. Box 9504, 2300 RA Leiden, The Netherlands.
Received February 28, 1992

Abstract: Ab-initio calculations at the UHF and CASSCF levels have been performed in which the geometry of pyrimidine in the $^3B_1(n\pi^*)$, $^3A_2(n\pi^*)$, and $^3A_1(\pi\pi^*)$ states has been optimized. The calculations clearly demonstrate the influence of vibronic coupling on the molecular and electronic structure of the molecule in these states. For the $n\pi^*$ states, conformations corresponding to minimum energy are found that deviate significantly from planar. For the $^3A_1(\pi\pi^*)$ state, vibronic coupling similar to that between the $^3B_{1u}$ and $^3E_{1u}$ states of benzene has been found. From the calculations, we deduce a dynamic out-of-plane distortion of the molecule in the $^3B_1(n\pi^*)$ state, which provides for a coherent description of the results of optical and magnetic-resonance data available for the lowest triplet state of pyrimidine. The out-of-plane distortions occurring in the $^3B_1(n\pi^*)$ and $^3A_2(n\pi^*)$ states conform to the increased antibonding character of the π-electron system upon $n\pi^*$ excitation.

Introduction

The class of azaaromatic molecules distinguishes itself from the hydrocarbon analogues by the presence of one or more nitrogen atoms in the conjugated system. The introduction of these nitrogen atoms leads to the occurrence of $n\pi^*$ excited states and modifies the electronic properties of the $\pi\pi^*$ excited states as compared to those of their hydrocarbon parent compounds. Extensive experimental and theoretical studies have been performed to characterize the low-lying excited states of azaaromatic compounds, as amply illustrated in a recent review.[1] For many such molecules, vibronic coupling has been invoked between $n\pi^*$ and $\pi\pi^*$ states as well as among $\pi\pi^*$ states in order to describe the properties of the excited states.

For pyridine, the simplest azaaromatic molecule, such studies have been problematic for a long time owing to its unfavorable emissive characteristics. Recently, we were able to unravel in great detail the molecular and electronic structure of pyridine in the lowest triplet state ($^3B_1(n\pi^*)$) by the application of electron spin echo (ESE) spectroscopy[2-5] and by ab-initio calculations.[6] From the observed nitrogen and deuterium hyperfine interactions, it was found that pyridine upon excitation adopts a boatlike structure in which the nitrogen and the para-carbon atoms are tilted by about 40 and 10°, respectively, with respect to the plane spanned by the ortho- and meta-carbon atoms. The nonplanar structure could be rationalized in terms of a strong vibronic coupling between the $^3B_1(n\pi^*)$ and $^3A_1(\pi\pi^*)$ states. In agreement with the vibronic coupling picture, the observed spin-density distribution reflected a state of both $n\pi^*$ and $\pi\pi^*$ character.

The experimentally determined molecular structure has subsequently beautifully been confirmed by theoretical studies performed by Nagaoka and Nagashima[7] and by us.[6] From our calculations, we concluded that the observed distortion could, besides in terms of vibronic coupling, be considered in terms of the increased antibonding character of the π-electron system upon $n\pi^*$ excitation. This suggested that the π^* orbital involved in the excitation might determine the character of the geometry relaxation. Indeed, our calculations showed that the nodal-plane structure of the $3b_1(\pi^*)$ orbital correlates very well with the way pyridine distorts in the lowest triplet state.

†University of California. Present address: Department of Physical Chemistry, University of Amsterdam, Nieuwe Achtergracht 127, 1018 WS Amsterdam, The Netherlands.
‡University of Leiden.

(1) Innes, K. K.; Ross, I. G.; Moomaw, W. R. *J. Mol. Spectrosc.* **1988**, *132*, 492.
(2) Bos, F. C.; Buma, W. J.; Schmidt, J. *Chem. Phys. Lett.* **1985**, *117*, 203.
(3) Buma, W. J.; Groenen, E. J. J.; Schmidt, J. *Chem. Phys. Lett.* **1986**, *127*, 189.
(4) Groenen, E. J. J.; Buma, W. J.; Schmidt, J. *Isr. J. Chem.* **1989**, *29*, 99.
(5) Buma, W. J.; Groenen, E. J. J.; Schmidt, J.; de Beer, R. *J. Chem. Phys.* **1989**, *91*, 6549.
(6) Buma, W. J.; Groenen, E. J. J.; van Hemert, M. C. *J. Am. Chem. Soc.* **1990**, *112*, 5447.
(7) Nagaoka, S.; Nagashima, U. *J. Phys. Chem.* **1990**, *94*, 4467.

0002-7863/92/1514-9544$03.00/0 © 1992 American Chemical Society

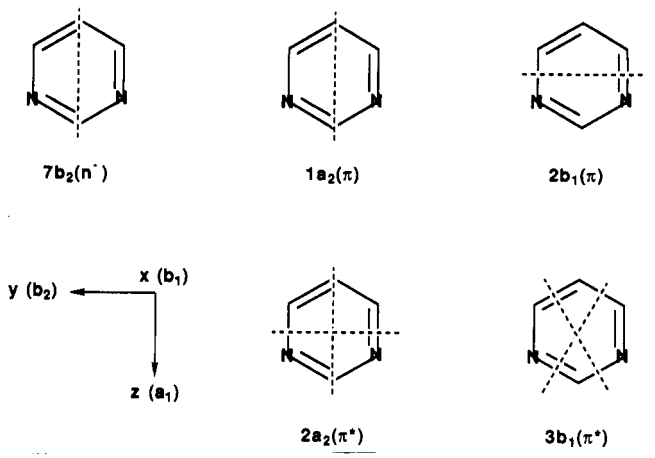

Figure 1. Relevant orbitals for the description of the lower triplet states of pyrimidine.

Apart from the vibronic coupling with $n\pi^*$ states, the $\pi\pi^*$ triplet states in azabenzenes may be subject to vibronic coupling with other $\pi\pi^*$ triplet states.[8] In azabenzenes, a low-lying $\pi\pi^*$ triplet state is present which is the analogue of the $^3B_{1u}$ state of benzene. This state has both experimentally[9-11] and theoretically[12-18] been shown to be subject to a large vibronic coupling with the $^3E_{1u}$ state of common MO parentage. As the result of this vibronic coupling, benzene in the $^3B_{1u}$ state is not stable in the D_{6h} conformation but distorts along the two-dimensional e_{2g} vibrational coordinate ν_8 in such a way that the potential energy surface of the $^3B_{1u}$ state exhibits a Mexican hat shape along ν_8. Within the trough of this surface, three equivalent minima and three equivalent saddle points can be found which correspond to quinoidal and antiquinoidal conformations. Recently, we investigated by ab-initio calculations the shape of the potential energy surface of the $^3B_{1u}$ state along the e_{2g} symmetry coordinate $S_8(\rho,\varphi)$.[17-19] The energy variation within the trough, i.e., the energy difference between quinoidal and antiquinoidal conformations, is found to be negligible compared to the stabilization energy that is gained by the distortion of the molecule from D_{6h} symmetry. Additionally, the calculation of vibronic energy levels and crystal fields supported the idea that the distortion of benzene in the $^3B_{1u}$ state is not a static process but a dynamic one.

In the present paper, we are concerned with the lower triplet states of pyrimidine (1,3-diazabenzene). By ab-initio calculations, we investigate the influence of vibronic coupling on the geometric and electronic structure of pyrimidine in the $^3B_1(n\pi^*)$, $^3A_2(n\pi^*)$, and $^3A_1(\pi\pi^*)$ states. The most relevant molecular orbitals for the description of these states are schematically indicated in Figure 1. The $^3B_1(n\pi^*)$ state can in first approximation be represented by the configuration $|7b_2(n^-) \rightarrow 2a_2(\pi^*)\rangle$, the $^3A_2(n\pi^*)$ state by $|7b_2(n^-) \rightarrow 3b_1(\pi^*)\rangle$, and the $^3A_1(\pi\pi^*)$ state by a mixture of the $|1a_2(\pi) \rightarrow 2a_2(\pi^*)\rangle$ and $|2b_1(\pi) \rightarrow 3b_1(\pi^*)\rangle$ configurations. The results of the calculations on the $n\pi^*$ states will be compared with those obtained for the lowest triplet state of pyridine. Especially interesting is the fact that the same π^* orbital is involved in the excitation to the $^3A_2(n\pi)^*$ state of pyrimidine as to the $^3B_1(n\pi^*)$ state of pyridine. The $^3A_1(\pi\pi^*)$ state, on the other hand, is the analogue of the $^3B_{1u}$ state of benzene. Calculations on this state allow for a discussion of the influence of the nitrogen atoms in the aromatic system on the vibronic coupling between $\pi\pi^*$ states.

The present calculations are of interest not only from a theoretical point of view but also in relation to the results of spectroscopic studies. Pyrimidine has a large phosphorescence quantum yield, and the lowest triplet state, $^3B_1(n\pi^*)$, has consequently been extensively studied by optical spectroscopy and optical detection of magnetic resonance. For the triplet manifold, vibronic coupling has repeatedly been invoked in order to explain experimental observations. The most salient among these observations concern the populating rates and the emission spectra of the sublevels of the lowest triplet state. Burland and Schmidt have observed that the populating rate of the T_x sublevel related to the out-of-plane axis is anomalously high.[20] Inoue and Lim rationalized this result by assuming a pseudo-Jahn–Teller distortion of pyrimidine in the $^3A_1(\pi\pi^*)$ and/or the $^3B_2(\pi\pi^*)$ state caused by a strong vibronic coupling with the $^3A_2(n\pi^*)$ state.[21] In addition, these authors suggested that the prominent presence of totally-symmetric bands in the emission spectrum of the T_x sublevel, which would be forbidden for a molecule of C_{2v} symmetry, is induced by an interplay of vibronic interactions and an anisotropic crystal field.[21] Hereby the molecule would acquire a symmetry lower than C_{2v} in the $^3B_1(n\pi^*)$ state. Nonhof and van der Waals inferred a similar symmetry lowering from optically-detected magnetic-resonance experiments in a magnetic field[22-24] and suggested vibronic coupling between the $^3B_1(n\pi^*)$ and $^3A_2(n\pi^*)$ states. Finally, the study of the polarization of bands in the T_x sublevel phosphorescence spectrum led Umemoto et al. to the conclusion that pyrimidine in the $^3B_1(n\pi^*)$ state is distorted along a b_1 vibrational coordinate, yielding a molecule of C_{1h} symmetry.[25] On the other hand, Donckers et al. concluded from a study of the nitrogen and proton hyperfine interactions in the $^3B_1(n\pi^*)$ state of pyrimidine present as a guest in a single crystal of benzene-d_6 that pyrimidine shows up as a planar molecule in the $^3B_1(n\pi^*)$ state on the time scale of their optically detected electron nuclear double resonance (ODENDOR) experiments.[26] They found no evidence for vibronic coupling with higher lying $^3\pi\pi^*$ states.

In our calculations, we have optimized the geometry of pyrimidine in the triplet states at the unrestricted Hartree–Fock (UHF) as well as the complete active space self-consistent field (CASSCF) level. The motivation for performing these two types of calculations stems from previous studies on the $^3B_1(n\pi^*)$ state of pyridine.[6,7] For this state, a qualitatively correct picture of the dominant geometry changes induced by the excitation was obtained already at the UHF level. The geometry optimizations of pyrimidine in the $^3B_1(n\pi^*)$, $^3A_2(n\pi^*)$, and $^3A_1(\pi\pi^*)$ states demonstrate that vibronic coupling is prominently present in the lower triplet manifold. The $^3B_1(n\pi^*)$ state is vibronically coupled to the $^3A_1(\pi\pi^*)$ state and has a nonplanar conformation at an energy of 68 cm^{-1} below that of the planar conformation. The $^3A_2(n\pi^*)$ state is even more perturbed by vibronic coupling with the $^3B_2(\pi\pi^*)$ state, resulting in an energy minimum for a nonplanar conformation at about 500 cm^{-1} below the planar conformation. The $^3A_1(\pi\pi^*)$ state exhibits similar in-plane deformations as previously encountered in the $^3B_{1u}$ state of benzene, albeit that the energy variations in the trough are considerably larger than the ones calculated for benzene. On the basis of the present calculations, we conclude that there is a dynamic out-of-plane distortion of pyrimidine in the lowest triplet state. Such a view offers a coherent explanation for the seemingly contra-

(8) McWeeny, R.; Peacock, T. E. *Proc. Phys. Soc* **1957**, *A70*, 41.
(9) de Groot, M. S.; van der Waals, J. H. *Mol. Phys.* **1963**, *6*, 545.
(10) Ponte Goncalves, A. M.; Hutchison, C. A., Jr. *J. Chem. Phys.* **1968**, *49*, 4235.
(11) Burland, D. M.; Castro, G.; Robinson, G. W. J. *J. Chem. Phys.* **1970**, *52*, 4100.
(12) Moffitt, W.; Liehr, A. D. *Phys. Rev.* **1957**, *106*, 1195.
(13) Liehr, A. D. *Z. Naturforsch.* **1961**, *16A*, 641.
(14) van der Waals, J. H.; Berghuis, A. M. D.; de Groot, M. S. *Mol. Phys.* **1967**, *13*, 301.
(15) van der Waals, J. H.; Berghuis, A. M. D.; de Groot, M. S. *Mol. Phys.* **1971**, *21*, 497.
(16) Osamura, Y. *Chem. Phys. Lett.* **1988**, *145*, 541.
(17) Buma, W. J.; van der Waals, J. H.; van Hemert, M. C. *J. Am. Chem. Soc.* **1989**, *111*, 86.
(18) Buma, W. J.; van der Waals, J. H.; van Hemert, M. C. *J. Chem. Phys.* **1990**, *93*, 3733.
(19) Buma, W. J.; van der Waals, J. H.; van Hemert, M. C. *J. Chem. Phys.* **1990**, *93*, 3746.
(20) Burland, D. M.; Schmidt, J. *Mol. Phys.* **1971**, *22*, 19.
(21) Inoue, A.; Lim, E. C. *Chem. Phys. Lett.* **1979**, *62*, 250.
(22) Nonhof, C. J.; van der Waals, J. H. *Chem. Phys. Lett.* **1982**, *92*, 581.
(23) Nonhof, C. J.; van der Waals, J. H. *Chem. Phys. Lett.* **1982**, *92*, 588.
(24) Nonhof, C. J. Ph.D. Thesis, University of Leiden, 1982.
(25) Umemoto, M.; Ogata, T.; Shimada, H.; Shimada, R. *Bull. Chem. Soc. Jpn.* **1984**, *57*, 3300.
(26) Donckers, M. C. J. M.; Gorcester, J.; Groenen, E. J. J.; Schmidt, J. *J. Chem. Phys.* **1992**, *97*, 99.

Table I. Optimized Geometries of Pyrimidine in the Ground State in Comparison with the Experimentally Determined Geometry[a]

	RHF	CASSCF	exptl[b]
energy	−262.564 48	−262.653 27	
C_5–C_6	1.385	1.395	1.393
C_6–N_1	1.334	1.346	1.350
N_1–C_2	1.330	1.342	1.328
C_5–H_9	1.070	1.071	1.087
C_6–H_{10}	1.070	1.070	1.079
C_2–H_7	1.067	1.066	1.082
C_6–C_5–C_4	116.9	117.4	117.8
C_5–C_6–N_1	121.4	121.2	121.2
C_6–N_1–C_2	117.7	117.7	116.0
N_1–C_2–N_3	124.8	124.8	128.0
H_9–C_5–C_6	121.5	121.3	121.1
H_{10}–C_6–C_5	121.9	121.2	120.9
H_{10}–C_6–N_1	116.7	116.6	117.9
H_7–C_2–N_1	117.6	117.6	116.0

[a] The energies are given in hartrees, the bond lengths in angstroms, and the bond angles in degrees. [b] From ref 28.

dictory results of optical and magnetic-resonance experiments. Finally, the calculated conformational behavior of pyrimidine in the $^3B_1(n\pi^*)$ and $^3A_2(n\pi^*)$ states will be considered in relation to previous theoretical results on the $^3B_1(n\pi^*)$ state of pyridine and described in relation to the nature of the molecular orbitals that participate in the electronic transition.

Computational Details

Ab-initio calculations have been performed using the GAMESS program package developed by Dupuis and co-workers,[27] employing the 6-31G basis set. Optimized geometries of pyrimidine have been calculated for the ground state and the lowest $^3B_1(n\pi^*)$, $^3A_2(n\pi^*)$, and $^3A_1(\pi\pi^*)$ states. Two approaches have been explored: In the first instance, the geometry of the molecule in the ground state and the triplet states has been optimized at the RHF and UHF levels of approximation, respectively. Subsequently, geometry optimizations have been performed using the CASSCF approach for the n- and π-electron molecular-orbital space. In the latter calculations, all possible configurations of the proper symmetry which arise from assigning the four n electrons and the six π electrons of pyrimidine to two nonbonding and six π molecular orbitals have been used to expand the electronic wave function. The geometry optimizations have been carried out using the energy-gradient technique.

Results

Our principal interest concerns the geometry changes of pyrimidine upon excitation from the ground state to the $^3B_1(n\pi^*)$, $^3A_2(n\pi^*)$, and $^3A_1(\pi\pi^*)$ states. In order to come to a meaningful discussion of these geometry changes, we have determined the equilibrium geometry of the molecule in its electronic ground state within the same computational strategy as applied for the triplet states. In Table I, we report the RHF- and CASSCF-optimized geometries of pyrimidine in its planar ground state for which energies of −262.564 48 and −262.653 27 hartrees have been calculated, respectively. These energies compare favorably with energies obtained in similar calculations with slightly larger basis sets for geometries that are in minor aspects different from the ones reported here.[29] Also given in this table is the geometry as determined experimentally on the basis of microwave, NMR, and electron-diffraction studies.[28] The CASSCF geometry is represented in Figure 2, in which also are given the numbering of the atoms and the definition of the axis system that will be used throughout this paper. The comparison of the RHF- with the CASSCF-optimized geometry shows that the inclusion of electron correlation does not influence the structural parameters to a large extent, the largest differences being of the order of 0.01 Å in the bond lengths and 0.5° in the bond angles. Calculated and experimental structures agree to a large extent, but the calculations underestimate the N_1–C_2–N_3 angle.

(27) Dupuis, M.; Spangler, D.; Wendolosky, J. J. *NRCC Software Catalog*; NRCC: Ottawa, 1980; Vol. 1, Program QC01 (GAMESS).
(28) Cradock, S.; Liescheski, P.; Rankin, D. W. H.; Robertson, H. E. *J. Am. Chem. Soc.* **1988**, *110*, 2758.
(29) Palmer, M.; Walker, I. C.; Guest, M. F.; Hopkirk, P. *Chem. Phys.* **1990**, *147*, 19.

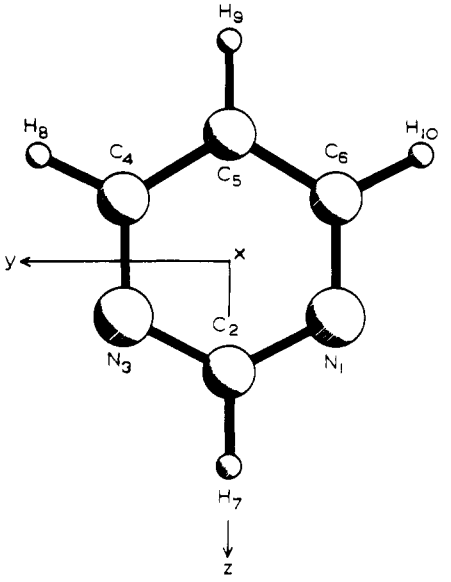

Figure 2. CASSCF-optimized geometry of pyrimidine in its ground state. Also given are the numbering of the atoms and the axis system used.

Table II. Optimized Geometries of Pyrimidine in the $^3B_1(n\pi^*)$ State[a]

	UHF (C_{2v})	CASSCF (C_{2v})	CASSCF (C_{1h})
energy	−262.430 82	−262.518 24	−262.518 55
C_5–C_6	1.390 (+0.005)	1.394 (−0.001)	1.394 (−0.001)
C_6–N_1	**1.406 (+0.072)**	**1.402 (+0.056)**	**1.414 (+0.068)**
N_1–C_2	1.316 (−0.014)	1.330 (−0.012)	1.335 (−0.007)
C_5–H_9	1.073 (+0.003)	1.072 (+0.001)	1.072 (+0.001)
C_6–H_{10}	1.066 (−0.004)	1.066 (−0.004)	1.066 (−0.004)
C_2–H_7	1.067	1.064 (−0.002)	1.065 (−0.001)
C_6–C_5–C_4	118.4 (+1.5)	118.9 (+1.5)	118.7 (+1.3)
C_5–C_6–N_1	117.9 (−3.5)	117.9 (−3.3)	118.6 (−2.6)
C_6–N_1–C_2	**124.3 (+6.6)**	**123.9 (+6.2)**	**121.9 (+4.2)**
N_1–C_2–N_3	**117.2 (−7.6)**	**117.4 (−7.4)**	**118.8 (−6.0)**
H_9–C_5–C_6	120.8 (−0.7)	120.5 (−0.8)	120.6 (−0.7)
H_{10}–C_6–C_5	125.7 (+3.8)	125.3 (+4.1)	125.1 (+3.9)
H_{10}–C_6–N_1	116.4 (−0.3)	116.8 (+0.2)	116.3 (−0.3)
H_7–C_2–N_1	121.4 (+3.8)	121.4 (+3.8)	120.1 (+2.5)
C_5–C_6–N_1–C_2			9.4
N_1–C_2–N_3–C_4			13.9
N_3–C_4–C_5–C_6			4.6
H_9–C_5–N_1–C_2			−179.9
H_{10}–C_6–N_1–C_2			−167.4
H_7–C_2–N_3–C_4			−177.3
H_8–C_4–C_5–C_6			−171.9

[a] The energies are given in hartrees, the bond lengths in angstroms, and the bond angles and dihedral angles in degrees. In parentheses is given the difference from the corresponding parameter in the ground state. For the UHF calculation, this difference concerns the RHF calculation for the ground state, and for the CASSCF calculation, the CASSCF calculation for the ground state. Those bond distances and bond angles that are subject to particularly large changes in comparison to the ground state are boldfaced.

The optimization of the geometry of pyrimidine in the $^3B_1(n\pi^*)$ state using the UHF method leads to a planar geometry of C_{2v} symmetry (Table II). The calculation of the force constant matrix in this geometry shows that the C_{2v} geometry corresponds to a stable minimum on the potential energy surface of the $^3B_1(n\pi^*)$ state at the UHF level. The comparison of the UHF-optimized geometry of pyrimidine in the $^3B_1(n\pi^*)$ state with the RHF-optimized geometry of pyrimidine in the ground state reveals that the significant geometry changes occur in the C_6–N_1 (C_4–N_3) bond length and the C_6–N_1–C_2 (C_4–N_3–C_2) and N_1–C_2–N_3 bond angles. Since the C_{2v} geometry of the $^3B_1(n\pi^*)$ state represents a stable minimum at the UHF level, we have in the first instance optimized the geometry at the CASSCF level under the constraint of C_{2v} symmetry (Table II). When we compare the CASSCF-optimized geometry with the analogous one of the ground state and consider those structural changes in relation to the ones found previously

Table III. Optimized Geometries of Pyrimidine in the $^3A_2(n\pi^*)$ State[a]

	UHF (C_{2v})	CASSCF (C_{2v})	UHF (C_{1h})	CASSCF (C_{1h})
energy	−262.415 27	−262.497 10	−262.420 70	−262.499 36
C_5–C_6	1.407 (+0.022)	1.411 (+0.016)	1.403 (+0.018)	1.407 (+0.012)
C_6–N_1	1.304 (−0.030)	1.320 (−0.026)	1.308 (−0.026)	1.321 (−0.025)
N_1–C_2	**1.403 (+0.073)**	**1.393 (+0.051)**	**1.416 (+0.086)**	**1.405 (+0.063)**
C_5–H_9	1.068 (−0.002)	1.068 (−0.003)	1.069 (−0.001)	1.069 (−0.002)
C_6–H_{10}	1.073 (+0.003)	1.070	1.073 (+0.003)	1.071 (+0.001)
C_2–H_7	1.057 (−0.010)	1.057 (−0.009)	1.067	1.064 (−0.002)
C_6–C_5–C_4	113.6 (−3.3)	115.1 (−2.3)	113.5 (−3.4)	114.9 (−2.5)
C_5–C_6–N_1	121.7 (+0.3)	120.8 (−0.4)	121.5 (+0.1)	120.9 (−0.3)
C_6–N_1–C_2	**126.9 (+9.2)**	**125.8 (+8.1)**	**127.8 (+10.1)**	**126.3 (+8.6)**
N_1–C_2–N_3	**109.2 (−15.6)**	**111.6 (−13.2)**	**106.6 (−18.2)**	**109.5 (−15.3)**
H_9–C_5–C_6	123.2 (+1.7)	122.5 (+1.2)	123.3 (+1.8)	122.5 (+1.2)
H_{10}–C_6–C_5	121.8 (−0.1)	122.6 (+1.4)	122.0 (+0.1)	122.6 (+1.4)
H_{10}–C_6–N_1	116.5 (−0.2)	116.6	116.5 (−0.2)	116.5 (−0.1)
H_7–C_2–N_1	**124.4 (+7.8)**	**124.2 (+6.6)**	118.0 (+0.4)	119.4 (+1.8)
C_5–C_6–N_1–C_2			−8.1	−6.5
N_1–C_2–N_3–C_4			−11.5	−12.0
N_3–C_4–C_5–C_6			−2.4	0.8
H_9–C_5–N_1–C_2			−178.4	−179.3
H_{10}–C_6–N_1–C_2			172.1	174.2
H_7–C_2–N_3–C_4			−147.1	−154.9
H_8–C_4–C_5–C_6			−177.6	−178.5

[a] Format as given in the footnote to Table II.

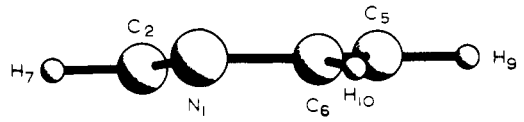

Figure 3. CASSCF-optimized geometry of pyrimidine in the $^3B_1(n\pi^*)$ state under the restriction of C_{1h} symmetry. The conformation has been drawn as a projection on the *zx* plane.

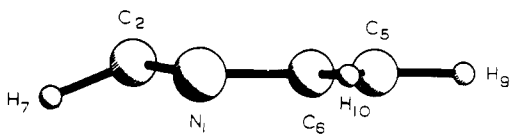

Figure 4. CASSCF-optimized geometry of pyrimidine in the $^3A_2(n\pi^*)$ state under the restriction of C_{1h} symmetry. The conformation has been drawn as a projection on the *xz* plane.

at the UHF/RHF level, we observe basically the same changes, albeit slightly smaller. Calculation of the force constant matrix for the CASSCF C_{2v} geometry of the $^3B_1(n\pi^*)$ state gives rise however to one imaginary frequency, indicative of the instability of this conformation at the CASSCF level. The coordinate associated with this imaginary frequency is an out-of-plane one of b_1 symmetry which lowers the symmetry of the molecule from C_{2v} to C_{1h}, the reflection plane being the *zx* plane. The subsequent optimization of the geometry within C_{1h} symmetry leads to a minimum corresponding to a nonplanar geometry for pyrimidine in the $^3B_1(n\pi^*)$ state at an energy 68 cm^{-1} below that of the corresponding state in the C_{2v} geometry. The structural parameters of this conformation are given in Table II, while the projection of the geometry on the *zx* plane is drawn in Figure 3. The main deviations from planarity concern the position of the C_2 and the H_{10} (H_8) atoms with respect to the plane defined by C_6–N_1–N_3–C_4. The projection of the $N_1(N_3)$–C_2 bond on the *zx* plane makes an angle of about 10° with the *z* axis, while the analogous projection of the C_6–H_{10} (C_4–H_8) bond makes an angle of about 13° with this axis. We notice that the C_2–H_7 bond remains nearly parallel to the C_6–N_1–N_3–C_4 plane. The rest of the molecule is to a good approximation still planar. As compared to the ground-state geometry, the changes in bond lengths and bond angles are qualitatively similar for the optimized geometries of pyrimidine in the $^3B_1(n\pi^*)$ state under C_{2v} and C_{1h} symmetries.

The geometry optimization of pyrimidine in the $^3A_2(n\pi^*)$ state has been performed analogously to that for the $^3B_1(n\pi^*)$ state. First, the geometry of the molecule has been optimized within C_{2v} symmetry at the UHF and CASSCF levels, leading to the geometries given in Table III. For the $^3A_2(n\pi^*)$ state, as compared to the ground state, especially the N_1–C_2 (N_3–C_2) bond lengthens, the C_6–N_1–C_2 (C_4–N_3–C_2) bond angle increases, and the N_1–C_2–N_3 bond angle decreases (with a concurrent increase of the H_7–C_2–N_1 (H_7–C_2–N_3) bond angle). The force constant matrices calculated for the UHF- and CASSCF-optimized geometries demonstrate that these planar geometries of C_{2v} symmetry do not represent true minima on the potential energy surface of the $^3A_2(n\pi^*)$ state but should be considered as saddle points because one of the normal modes gives rise to an imaginary frequency in both calculations. The coordinate belonging to this frequency is once again an out-of-plane coordinate of b_1 symmetry distorting the molecule from C_{2v} to C_{1h} symmetry, the *zx* plane remaining the plane of symmetry. The optimization of the geometry under the constraint of C_{1h} symmetry results in the stable geometries at the UHF and CASSCF levels given in Table III. The corresponding UHF and CASSCF energies imply stabilizations with respect to the C_{2v} conformation of 1192 and 495 cm^{-1}, respectively. A projection for the CASSCF-optimized structure on the *zx* plane is represented in Figure 4. Particularly significant is the position of the C_2–H_7 fragment with respect to the rest of the molecule. The projection of the N_1–C_2 (N_3–C_2) bond on the *zx* plane makes an angle with the *z* axis of 8° (9°) in the UHF (CASSCF) calculation, while the C_2–H_7 bond makes an angle of −29° (−23°) with that axis. The comparison of the bond lengths and bond angles in the two optimized geometries with those in the ground state shows similar changes, as previously observed for the C_{2v} conformations of the $^3A_2(n\pi^*)$ state. The notable exception is the H_7–C_2–N_1 (H_7–C_2–N_3) bond angle which, as the result of the out-of-plane distortion of the C_2–H_7 fragment, becomes almost equal to that in the ground state.

Finally, we consider the calculations on the geometry of pyrimidine in the $^3A_1(\pi\pi^*)$ state. Since, in the present case, we are interested in the analogies with the in-plane deformations as they occur in the $^3B_{1u}$ state of benzene, we make use of the terminology associated with the ν_8 vibration. This vibration is a degenerate vibration which can be expressed in the polar coordinates ρ and φ. In the definition used previously,[17,18] the quinoidal conformations occur for φ = 0, 120, and 240°, while the antiquinoidal conformations occur for φ = 60, 180, and 300°. In pyrimidine, the conformations with φ = 120 and 240° are due to symmetry of the same energy. Likewise, the conformations with φ = 60 and 300° will be of the same energy. We have performed the geometry optimizations of pyrimidine in the $^3A_1(\pi\pi^*)$ state under the restriction of C_{1h} symmetry with the *zy* plane as the plane of symmetry. On this cross section of the potential energy surface, we indeed find at the UHF level three minima and three saddle points of which the geometries are given in Table IV. The conformations that roughly can be described as corresponding to the antiquinoidal

Table IV. Optimized Geometries for Pyrimidine in the $^3A_1(\pi\pi^*)$ State[a]

(a) Quinoidal Geometry Corresponding to $\varphi = 0°$ and Antiquinoidal Geometry Corresponding to $\varphi = 180°$

	UHF ($\varphi = 0°$)	CASSCF ($\varphi = 0°$)	UHF ($\varphi = 180°$)	CASSCF ($\varphi = 180°$)
energy	−262.448 87	−262.520 03	−262.460 99	−262.515 37
C_5–C_6	**1.518 (+0.133)**	**1.470 (+0.075)**	1.386 (+0.001)	1.396 (+0.001)
C_6–N_1	**1.295 (−0.039)**	**1.305 (−0.041)**	**1.486 (+0.152)**	**1.458 (+0.112)**
N_1–C_2	**1.386 (+0.056)**	**1.422 (+0.080)**	1.340 (+0.010)	1.348 (+0.006)
C_5–H_9	1.069 (−0.001)	1.068 (−0.003)	1.073 (+0.003)	1.072 (+0.001)
C_6–H_{10}	1.071 (+0.001)	1.070	1.067 (−0.003)	1.066 (−0.004)
C_2–H_7	1.064 (−0.003)	1.057 (−0.009)	1.069 (+0.002)	1.068 (+0.002)
C_6–C_5–C_4	114.2 (−2.7)	116.9 (−0.5)	119.6 (+2.7)	119.8 (+2.4)
C_5–C_6–N_1	120.8 (−0.6)	121.6 (+0.4)	120.2 (−1.2)	120.3 (−0.9)
C_6–N_1–C_2	119.9 (+2.2)	118.0 (+0.3)	116.8 (−0.9)	117.0 (−0.7)
N_1–C_2–N_3	124.4 (−0.4)	123.8 (−1.0)	126.5 (+1.7)	126.2 (+1.4)
H_9–C_5–C_6	122.9 (+1.4)	121.5 (+0.2)	120.2 (−1.3)	120.4 (−0.9)
H_{10}–C_6–C_5	120.3 (−1.6)	120.5 (−0.7)	125.3 (+3.4)	124.6 (+3.4)
H_{10}–C_6–N_1	118.9 (+2.2)	117.9 (+1.3)	114.5 (−2.2)	115.0 (−1.6)
H_7–C_2–N_1	117.8 (+0.2)	118.1 (+0.5)	116.8 (−0.8)	116.9 (−0.7)

(b) Quinoidal Geometry Corresponding to $\varphi = 120°$ and Antiquinoidal Geometry Corresponding to $\varphi = 60°$

	UHF ($\varphi = 120°$)	CASSCF ($\varphi = 120°$)	UHF ($\varphi = 60°$)
energy	−262.451 63	−262.517 16	−262.463 32
C_5–C_6	**1.348 (−0.037)**	**1.365 (−0.030)**	**1.520 (+0.135)**
C_5–C_4	**1.438 (+0.053)**	**1.473 (+0.127)**	1.388 (+0.003)
C_6–N_1	**1.482 (+0.148)**	**1.411 (+0.065)**	1.335 (+0.001)
C_4–N_3	**1.397 (+0.063)**	**1.408 (+0.066)**	1.344 (+0.010)
N_1–C_2	**1.496 (+0.166)**	**1.446 (+0.104)**	1.328 (−0.002)
N_3–C_2	**1.295 (−0.035)**	**1.302 (−0.040)**	**1.491 (+0.161)**
C_5–H_9	1.072 (+0.002)	1.071	1.070
C_6–H_{10}	1.068 (−0.002)	1.069 (−0.001)	1.068 (−0.002)
C_4–H_8	1.068 (−0.002)	1.066 (−0.004)	1.072 (+0.002)
C_2–H_7	1.067	1.066	1.065 (−0.002)
C_6–C_5–C_4	120.4 (+3.5)	118.8 (+1.4)	117.8 (+0.9)
C_5–C_6–N_1	121.1 (−0.3)	121.8 (+0.6)	119.5 (−1.9)
C_5–C_4–N_3	120.8 (−0.6)	119.5 (−1.7)	122.8 (+1.4)
C_6–N_1–C_2	112.8 (−4.9)	115.7 (−2.0)	119.7 (+2.0)
C_4–N_3–C_2	120.0 (+2.3)	118.7 (+1.0)	115.7 (−2.0)
N_1–C_2–N_3	124.9 (+0.1)	125.6 (+0.8)	124.4 (−0.4)
H_9–C_5–C_6	120.4 (−1.1)	121.5 (+0.2)	120.1 (−1.4)
H_9–C_5–C_4	119.2 (−2.3)	119.8 (−1.5)	122.1 (+0.6)
H_{10}–C_6–C_5	124.7 (+2.8)	123.1 (+1.9)	121.6 (−0.3)
H_8–C_4–C_5	122.5 (+0.6)	123.5 (+2.3)	121.1 (−0.8)
H_{10}–C_6–N_1	114.2 (−2.5)	115.1 (−1.5)	118.8 (+2.1)
H_8–C_4–N_3	116.7	117.0 (+0.4)	116.2 (−0.5)
H_7–C_2–N_1	114.2 (−3.4)	114.8 (−2.8)	120.5 (+2.9)
H_7–C_2–N_3	120.9 (+3.3)	119.7 (+2.1)	115.1 (−2.5)

[a] Format as given in the footnote to Table II.

conformations constitute at the UHF level the true minima, while the quinoidal conformations represent the saddle points in the trough. As will become clear from the following, the influence of the electron correlation on the geometry and relative energies of the various conformations in the $^3A_1(\pi\pi^*)$ state is much larger than for the $n\pi^*$ states. For this reason we will at this point not consider the geometry changes with respect to the ground state.

On the CASSCF level, the ordering in energy of the quinoidal and antiquinoidal conformations is reversed and even the mutual ordering of the three quinoidal conformations is changed. At this level, we have been able to locate four of the six conformations: the quinoidal conformations corresponding to $\varphi = 0°$ and $\varphi = 120°$ (240°) and one of the antiquinoidal conformations, namely the one corresponding to $\varphi = 180°$. The geometries are given in Table IV. In the $^3A_1(\pi\pi^*)$ state, the $\varphi = 0°$ conformation is now the one of lowest energy while the conformation corresponding to $\varphi = 120°$ (240°) is found 630 cm^{-1} higher in energy. The conformation corresponding to $\varphi = 180°$ represents a saddle point, 1022 and 392 cm^{-1} higher in energy than the minima obtained at $\varphi = 0°$ and $\varphi = 120°$ (240°), respectively. As compared to the ground-state geometry, the main changes occur for the $\varphi = 0°$ conformation in the bond length C_6–N_1 (C_4–N_3), which is shortened, and the C_5–C_6 (C_5–C_4) and N_1–C_2 (N_3–C_2) bond lengths, which are elongated; for the $\varphi = 120°$ conformation, the bond lengths C_5–C_6 and N_3–C_2 are shortened while C_6–N_1, C_4–N_3, N_1–C_2, and C_4–C_5 are elongated, and for the $\varphi = 180°$ conformation, the C_6–N_1 (C_4–N_3) bond is elongated.

Table V. Vertical and Relaxed Excitation Energies (eV) of the $^3B_1(n\pi^*)$, $^3A_1(\pi\pi^*)$, and $^3A_2(n\pi^*)$ states

	C_{2v} (vertical[a])	C_{2v} (relaxed[b])	C_{1h} (relaxed[c])	C_{2v} (vertical[d])
$^3B_1(n\pi^*)$	4.072	3.674	3.666	3.684
$^3A_1(\pi\pi^*)$[e]	4.017	3.626		3.895
$^3A_2(n\pi^*)$	4.781	4.250	4.188	3.899

[a] Vertical excitation energy based on the CASSCF energies of the triplet states in the CASSCF-optimized geometry of the ground state. [b] Relaxed excitation energy based on the CASSCF energies of the C_{2v} optimized geometries of the ground and triplet states. [c] Relaxed excitation energy based on the CASSCF energies of the C_{1h} optimized geometries of the triplet states and the C_{2v} optimized ground state. [d] Vertical excitation energies according to ab-initio calculations of Palmer et al.[29] [e] $\varphi = 0°$.

Discussion

We first consider the relative ordering of the various triplet states. In Table V, we summarize the calculated vertical and relaxed excitation energies of the triplet states investigated here and compare these energies with the values obtained in the most extensive ab-initio calculations performed as yet.[29] Experimental studies of the lowest triplet state of pyrimidine in the solid state[20] and in the gas phase[30] have established the $^3B_1(n\pi^*)$ character

(30) Fujita, M.; Ohta, N.; Takemura, T.; Baba, H. *Bull. Chem. Soc. Jpn.* **1988**, *61*, 1787.

of this state. Our calculations fail to reproduce the energy ordering of the triplet states, since we find the $^3A_1(\pi\pi^*)$ state lowest in energy, albeit that the calculated energy difference between the $^3A_1(\pi\pi^*)$ and $^3B_1(n\pi^*)$ states is very small. In the calculations of Palmer et al.,[29] in which up to 30 electrons were correlated, the $^3A_1(\pi\pi^*)$ and $^3B_1(n\pi^*)$ states appear in proper order. Our failure is probably due to the fact that only 10 electrons have been correlated in the present calculations. A partial justification for this hypothesis can be found in recent calculations of the excitation energies of the $^3B_1(n\pi^*)$ and $^3A_1(\pi\pi^*)$ states of pyridine.[31] Here the $^3A_1(\pi\pi^*)$ state has been calculated to be the lowest triplet state with an energy separation from the $^3B_1(n\pi^*)$ state that changes from 1.24 eV when only the n and π electrons are correlated to 0.15 eV when the σ electrons are also taken into account. Consequently, it is to be expected that also in the present calculations the inclusion of more electrons and molecular orbitals in the treatment of the electron correlation may lower the energy of the $^3B_1(n\pi^*)$ state more than that of the $^3A_1(\pi\pi^*)$ state.

The geometry optimization for pyrimidine in the $^3B_1(n\pi^*)$ state resulted at the UHF level in a planar conformation with C_{2v} symmetry, while at the CASSCF level an out-of-plane distorted conformation with C_{1h} symmetry was obtained that is 68 cm^{-1} more stable than the CASSCF-optimized conformation with C_{2v} symmetry. The difference between the results at the two levels of calculation underlines the important role of electron correlation. The magnitude of the stabilization energy should consequently be considered with caution, since it may depend largely on the amount of electron correlation taken into account and the size of the basis set. For the $^3A_2(n\pi^*)$ state, the geometry optimization resulted at both levels in an out-of-plane distorted conformation. Electron correlation is also important for this state: at the UHF level a stabilization energy of 1192 cm^{-1} has been calculated, while at the CASSCF level this energy is reduced to 495 cm^{-1}. It can be concluded that the stabilization energy corresponding to the out-of-plane distortion of the molecule in the $^3B_1(n\pi^*)$ state is small and is certainly not as large as that in the $^3A_2(n\pi^*)$ state.

We now compare the results of the calculations on the $^3B_1(n\pi^*)$ state with the available experimental data. In the optical studies, it has been observed that the 0–0 transition and the transitions involving totally-symmetric vibrations are prominently present in the emission spectrum of the T_x spin sublevel.[21-23,25] Such transitions would be forbidden if the molecule would retain C_{2v} symmetry in the $^3B_1(n\pi^*)$ state. Additionally, these transitions are found to be polarized analogously to the b_1 vibronic transitions and likewise the a_2 and b_2 vibronic transitions are found to be analogously polarized.[25] These observations have been taken as evidence for a distortion of the molecule in the $^3B_1(n\pi^*)$ state along a b_1 coordinate.[25] This conclusion seems to be in conflict with the results of ODENDOR experiments on the $^3B_1(n\pi^*)$ state. These studies have enabled an accurate determination of the hyperfine tensors of the nitrogen and hydrogen atoms.[26] The interpretation of these tensors has led to the conclusion that the molecule retains to a very good approximation its C_{2v} symmetry upon excitation; i.e., the molecule is not statically distorted in the $^3B_1(n\pi^*)$ state.

The conclusions drawn from the optical and the magnetic-resonance experiments are not as much in conflict as might at first seem; both conform to the picture arising from our calculations. According to the calculations, the potential energy surface of the $^3B_1(n\pi^*)$ state exhibits a double-minimum shape along one of the normal coordinates of b_1 symmetry. The two minima, of equal energy for the free molecule, are separated from each other by a barrier of 68 cm^{-1}, which corresponds to the planar conformation of pyrimidine. From the height of the barrier, we can safely infer that the zero-point vibrational level of the molecule in the $^3B_1(n\pi^*)$ state, the level investigated experimentally, is well above the barrier. As a result of the low barrier, the molecule is not statically distorted and, on the time scale of the ODENDOR experiments, the molecule will appear to be planar. On the other hand, owing to the double-minimum potential, the vibrational wave function of the zero-point level will have significant amplitude outside the C_{2v} conformation, where the selection rules become relaxed. After the proper average of the electronic transition moments over the various conformations is taken, the net result may be that in experiments based on the emissive character of the $^3B_1(n\pi^*)$ state the molecule appears to be distorted along a coordinate of b_1 symmetry. Equivalently, we can say that as the result of the vibronic coupling between the $^3B_1(n\pi^*)$ state and a higher lying triplet state, which is responsible for the presence of the double-minimum potential, vibronic intensity is induced in otherwise forbidden transitions and polarization rules are relaxed. We conclude that the experimental findings concerning the geometry of pyrimidine in the $^3B_1(n\pi^*)$ state can consistently be interpreted by a dynamic out-of-plane distortion of the molecule, in agreement with the results of our calculations which predict such a behavior.

Contrary to the out-of-plane distortion, in-plane geometry changes in the $^3B_1(n\pi^*)$ state as compared to the ground state do show up in the ODENDOR experiments. According to the interpretation of the magnetic-resonance data, the bond lengths C_6–N_1 (C_4–N_3) and N_1–C_2 (N_3–C_2) become larger and smaller, respectively, and the bond angle C_6–N_1–C_2 (C_4–N_3–C_2) becomes larger for the $^3B_1(n\pi^*)$ state. In both the C_{2v}- and C_{1h}-optimized geometries, the calculations reproduce these structural changes.

According to our calculations, the energy of the $^3B_1(n\pi^*)$ state is lowered upon a distortion of the molecule from C_{2v} symmetry along a b_1 vibrational coordinate. In terms of vibronic coupling, this implies that the $^3B_1(n\pi^*)$ state is coupled to a $^3A_1$ state which most likely is the second triplet state $1^3A_1(\pi\pi^*)$. According to the calculations of Palmer et al.,[29] this state is only 0.2 eV above the $^3B_1(n\pi^*)$ state, which makes such vibronic coupling likely from an energy point of view. This coupling is borne out from our calculations as well. In C_{2v} symmetry, the CASSCF wave function is given by $0.90|7b_2(n^-) \rightarrow 2a_2(\pi^*)\rangle + ...$, while for the optimized C_{1h} conformation substantial $1^3A_1(\pi\pi^*)$ character turns out to be mixed in since the CASSCF wave function is given by $0.80|7b_2(n^-) \rightarrow 2a_2(\pi^*)\rangle + 0.40|1a_2(\pi) \rightarrow 2a_2(\pi^*)\rangle + ...$

For the $^3A_2(n\pi^*)$ state of pyrimidine, experimental data are not available. From a theoretical point of view, it is of interest to compare this state with the $^3B_1(n\pi^*)$ state of pyridine. Both for the $^3A_2(n\pi^*)$ state of pyrimidine and for the $^3B_1(n\pi^*)$ state of pyridine, the excitation in first approximation corresponds to the promotion of an electron from a lone-pair orbital to the $3b_1(\pi^*)$ orbital. Recent ESE experiments and ab-inito calculations on the $^3B_1(n\pi^*)$ state of pyridine show that the molecule adopts a boatlike structure in which the nitrogen atom is tilted by about 40° and the para-carbon atom by about 10° with respect to the plane defined by the ortho- and meta-carbon atoms. Intimately related with this geometry change is a rehybridization of the ortho-carbon atoms which become almost sp^3 hybridized. The nitrogen atom retains, on the contrary, the sp^2 hybridization it has in the ground state. The present calculations show qualitatively a similar behavior for the $^3A_2(n\pi^*)$ state of pyrimidine. The molecule is unstable in the planar geometry and turns out to be out-of-plane distorted along a b_1 vibrational coordinate in both the UHF and CASSCF calculations. Whereas the stabilization energy depends on the level of calculation, the calculated optimized geometry hardly does. This has also been observed in the previous calculations on the $^3B_1(n\pi^*)$ state of pyridine.[6,7] In addition, also for the $^3A_2(n\pi^*)$ state of pyrimidine, the hybridization of the carbon atom next to the nitrogen (actually two nitrogens in this case) changes basically toward sp^3, as can be deduced from the fact that the N_1–C_2–N_3 bond angle is reduced from 125° in the ground state to 110° in the optimized geometry of the $^3A_2(n\pi^*)$ state.

A final point of interest concerns the state to which the $^3A_2(n\pi^*)$ state is vibronically coupled. The b_1 coordinate points to a $^3B_2$ partner, most probably the $1^3B_2(\pi\pi^*)$ state which, according to the calculations of Palmer et al.,[29] is about 0.8 eV higher in energy than the $^3A_2(n\pi^*)$ state. In the CASSCF wave function, however, such a mixing of the $^3A_2(n\pi^*)$ and $^3B_2(\pi\pi^*)$ states is not obvious, since a comparison of the wave functions in C_{2v} and C_{1h} symmetries does not reveal significant additional configurations in the C_{1h}

(31) Kitao, O.; Nakatsuji, H. *J. Chem. Phys.* **1988**, *88*, 4913.

wave function. Apparently, the effects of the vibronic coupling are already incorporated at the orbital level. We notice the conclusion that the $^3A_2(n\pi^*)$ state is coupled to the $^3B_2(\pi\pi^*)$ state implies that the $^3A_2(n\pi^*)$ state of pyrimidine and the $^3B_1(n\pi^*)$ state of pyridine are subject to a vibronic coupling with basically different $\pi\pi^*$ states. In pyridine, the vibronic coupling takes place with the $\pi\pi^*$ state of MO parentage similar to that of the $^3B_{1u}$ state of benzene. In pyrimidine, the vibronic coupling takes place with the $\pi\pi^*$ state of MO parentage similar to that of the $^3B_{2u}$ state of benzene.

The above discussed results of the calculations on the $^3B_1(n\pi^*)$ state and $^3A_2(n\pi^*)$ state have shown in which aspects pyrimidine is subject to conformational changes upon excitation to either one of these $n\pi^*$ states. In a coarse interpretation, one could say that the molecule undergoes the same type of structural changes in the sense that for both states distortions to out-of-plane geometries are calculated at the CASSCF level. The finer details of these out-of-plane changes are however markedly different for the two states. Excitation to the $^3B_1(n\pi^*)$ state brings about a relatively small out-of-plane distortion of the C_2–H_7 and C_6–H_{10} (C_4–H_8) fragments with such a small stabilization energy with respect to the C_{2v} geometry that explicit electron correlation is necessary for this out-of-plane distortion to show up. The excitation to the $^3A_2(n\pi^*)$ state, on the other hand, results in a large out-of-plane distortion of the C_2–H_7 fragment with a large stabilization energy, indicating that the vibronic coupling between the $^3A_2(n\pi^*)$ and $^3B_2(\pi\pi^*)$ states is considerably stronger than the vibronic coupling between the $^3B_1(n\pi^*)$ and $^3A_1(\pi\pi^*)$ states.

Apart from a description of the geometry changes occurring upon excitation to the $n\pi^*$ states in terms of vibronic coupling, it is instructive to consider these changes from the point of view of the electronic structure, as in our previous theoretical study of the $^3B_1(n\pi^*)$ state of pyridine.[6] We argued that an azabenzene in an $n\pi^*$ state may well be susceptible to out-of-plane distortions because the π-electron system in this kind of molecules becomes in first approximation a 7-π-electron system and thus is no longer aromatic. Because it is the excited electron that reduces the stabilization energy, we speculated that the kind of distortion the molecule undergoes might be intimately connected with the nature of the π^* orbital involved in the excitation. Such a reasoning adequately described the observations for pyridine. The present results on the $n\pi^*$ states of pyrimidine show that the geometry changes conform to the nature of the π^* orbital in this case as well. For the $^3B_1(n\pi^*)$ state, an electron is excited to the $2a_2(\pi^*)$ orbital, which is characterized by its antibonding character between the C_6 (C_4) and N_1 (N_3) atoms (see Figure 1). On the basis of the idea that the molecule will respond to this excitation in such a way as to reduce this antibonding character, we expect the major geometry changes to occur in the bonding between these atoms. Indeed it is seen that the bond between C_6 (C_4) and N_1 (N_3) is elongated, while an out-of-plane distortion occurs related to a rehybridization of the corresponding atomic orbitals. The latter geometry change results in only a small energy lowering of the $^3B_1(n\pi^*)$ state. For the $^3A_2(n\pi^*)$ state, an electron is excited to the $3b_1(\pi^*)$ orbital which is antibonding between C_5 and C_6 (C_4) and between C_2 and N_1 (N_3) (see Figure 1). In agreement with the above reasoning, we observe in this state an increase of the bond length between C_5 and C_6 (C_4) and especially between C_2 and N_1 (N_3), while in addition a strong out-of-plane distortion of the C_2–H_7 fragment takes place. This out-of-plane distortion does lower the energy of the $^3A_2(n\pi^*)$ state significantly.

The observed geometry changes in the $^3B_1(n\pi^*)$ state of pyridine and the $^3B_1(n\pi^*)$ and $^3A_2(n\pi^*)$ states of pyrimidine consequently seem to suggest that the geometry of the molecule is modified in a way that reduces the antibonding character of the excited-state wave function. For all of these states, this is accomplished partly by bond elongation (see also ref 7) and partly by an out-of-plane distortion of the molecule. For another diazabenzene, pyrazine, the lowest triplet state basically derives from the excitation of an electron from a lone-pair orbital into the $3b_{3u}(\pi^*)$ orbital (in D_{2h} symmetry). Since the latter orbital is the analogue of the $3b_1(\pi^*)$ orbital for pyridine and pyrimidine, one might expect a tendency toward elongation of the bonds between the carbon and nitrogen atoms and/or nonplanarity. Calculations by Ellenbogen et al.[32] on the planar pyrazine molecule of D_{2h} symmetry showed a lengthening of the carbon–nitrogen bonds, in agreement with the antibonding character of this bond in the $3b_{3u}(\pi^*)$ orbital. Magnetic-resonance experiments[33] do not support this observation and, moreover, conclusively demonstrate that pyrazine retains its D_{2h} symmetry upon excitation into the lowest triplet state on the time scale of the ODENDOR experiment. Whether this symmetric conformation corresponds to a minimum on the potential energy surface or whether it is observed as the result of a dynamic distortion cannot be concluded as yet and deserves further theoretical attention.

Our calculations on the $^3A_1(\pi\pi^*)$ state of pyrimidine have shown that vibronic coupling for this state can be compared with that for the $^3B_{1u}$ state of benzene. In benzene, vibronic coupling between the $^3B_{1u}$ and $^3E_{1u}$ states is responsible for in-plane deformations of the molecule in the $^3B_{1u}$ state. A potential energy surface has been calculated with a trough corresponding to quinoidal and antiquinoidal conformations of almost equal energies. For the $^3A_1(\pi\pi^*)$ state of pyrimidine, we find that the quinoidal conformations represent stable minima, while the antiquinoidal conformations are saddle points on the potential energy surface. A comparison of the energies of the three quinoidal conformations shows that the equivalence of these conformations, present in benzene because of symmetry, is lost: the conformation corresponding to $\varphi = 0°$ is the one of lowest energy, while those corresponding to $\varphi = 120$ and 240° are found 630 cm^{-1} higher in energy. Additionally it is seen in Table IV that the description as quinoidal and antiquinoidal is an approximation. In the true symmetry coordinate $S_8(\rho,\varphi)$ of benzene, the changes in lengths of the bonds that are elongated in the quinoidal form are twice as small as the changes in the bond lengths that are shortened. The recent geometry optimizations of benzene in the $^3B_{1u}$ state of Osamura[16] show that the actual deformation is pretty well described by $S_8(\rho,\varphi)$. This is not the case for the $^3A_1(\pi\pi^*)$ state of pyrimidine. For $\varphi = 0°$, the short bonds are only shortened by 0.04 Å, while the long ones are elongated by 0.08 Å. Similarly, the $\varphi = 120°$ (240°) conformation shows such an asymmetry with shortenings of 0.03 and 0.04 Å and elongations of 0.13, 0.10, and 0.07 Å. The same deviations from the $S_8(\rho,\varphi)$ coordinate are present in the antiquinoidal conformation with $\varphi = 180°$. Here it is basically only the C_6–N_1 (C_4–N_3) bond length which changes upon excitation. With respect to the bond angles, we notice that none of the conformations given in Table IV exhibit significant differences as compared to the ground-state geometry. This conforms to the character of the S_8 coordinate, which merely involves changes in bond lengths. The observed conformational behavior of pyrimidine in the $^3A_1(\pi\pi^*)$ state agrees qualitatively well with the idea that the original vibronic coupling between the $^3B_{1u}$ and $^3E_{1u}$ states in benzene still persists in pyrimidine,[8] although the quantitative description is to a large extent affected by the introduction of the two nitrogen atoms in the aromatic system.

Conclusions

We have investigated the geometry changes in pyrimidine upon excitation to the $^3B_1(n\pi^*)$, $^3A_2(n\pi^*)$, and $^3A_1(\pi\pi^*)$ states by ab-initio calculations at the UHF and the CASSCF levels. Each of these states is found to be subject to a strong vibronic coupling. For the $^3B_1(n\pi^*)$ state, the conformation of minimum energy corresponds to a nonplanar molecule although the energy difference with the planar geometry is calculated to be only 68 cm^{-1}. From this we deduce a dynamic out-of-plane distortion of pyrimidine in the lowest triplet state which describes consistently the results of optical as well as magnetic-resonance experiments. Excellent agreement has been found between the characteristic in-plane geometry changes predicted by our calculations and observed in the ODENDOR experiments.

(32) Ellenbogen, J. C.; Feller, D.; Davidson, E. R. *J. Phys. Chem.* **1982**, *86*, 1583.
(33) Donckers, M. C. J. M.; Schwencke, A. M.; Groenen, E. J. J.; Schmidt, J. *J. Chem. Phys.* **1992**, *97*, 110.

The vibronic coupling between the $^3A_2(n\pi^*)$ and the $^3B_2(\pi\pi^*)$ states demonstrates, in contrast, a much larger influence on the out-of-plane susceptibility of the molecule. The energy minimum for the $^3A_2(n\pi^*)$ state corresponds to an out-of-plane conformation which is stabilized with respect to the planar conformation by about 500 cm^{-1} in the CASSCF calculation and by about 1200 cm^{-1} in the UHF calculation.

The $^3A_1(\pi\pi^*)$ state has been shown to be subject to a vibronic coupling which is qualitatively similar to that between the $^3B_{1u}$ and the $^3E_{1u}$ states of benzene. The effect of introducing two nitrogen atoms in the aromatic ring manifests itself most clearly in the stabilization of the quinoidal conformation corresponding to $\varphi = 0°$; the other two quinoidal conformations are 630 cm^{-1} higher in energy, while the antiquinoidal conformations form the saddle points in the trough.

Finally, we have considered the description of the geometry changes in the $n\pi^*$ states in relation to the nature of the π^* orbital to which a lone-pair electron is in first approximation excited. Taking into account as well previous results on the $^3B_1(n\pi^*)$ state of pyridine, it has been shown that the structural response of the molecule to an $n\pi^*$ excitation correlates remarkably well with the nodal-plane structure of the π^* orbital. This structural response shows up partly in the elongation of bonds and partly in out-of-plane distortions. Though an $n\pi^*$ state in azabenzenes by its intrinsic nature seems to be susceptible to out-of-plane deformations, the contribution of such out-of-plane distortions to the total geometry relaxation does not have to dominate the structural response to the excitation.

Acknowledgment. This work was supported by The Netherlands Foundation for Chemical Research (SON) with financial aid from The Netherlands Organization for Scientific Research (NWO). W.J.B. acknowledges the San Diego Supercomputer Center (SDSC) for a grant of computer time on the CRAY-YMP, The Netherlands Organization for Scientific Research (NWO) for a research fellowship, and the Koninklijke/Shell Co. for the award of a bursary. This work was completed while W.J.B. was a postdoctoral fellow in the group of Prof. Dr. B. E. Kohler at the University of California, Riverside.

Registry No. Pyrimidine, 289-95-2.

Clusters of Phosphorus: A Theoretical Investigation

Marco Häser, Uwe Schneider, and Reinhart Ahlrichs*

Contribution from the Institut für Physikalische Chemie u. Elektrochemie, Lehrstuhl für Theoretische Chemie, Universität Karlsruhe, Kaiserstrasse 12, D-W-7500 Karlsruhe, Germany.
Received April 24, 1992

Abstract: A variety of phosphorus clusters up to P_{28} has been studied with ab initio SCF and MP2 calculations. Many of the larger clusters are found to be energetically stable with respect to P_4. The more interesting clusters are characterized by their equilibrium structures and NMR chemical shieldings and partially characterized by vibrational spectra to facilitate detection of the molecules. A probable reaction scheme for the formation of red phosphorus from white phosphorus emerges, and possible structural units of red phosphorus are established.

I. Introduction

"Precise molecular structure data for the various forms (of phosphorus) is still limited and although their inter-conversion can, in most cases, be carried out, many of the phenomena involved remain imperfectly understood".[1] Some of these gaps can now be filled with results from large-scale ab initio calculations. Previous attempts were directed toward small clusters up to P_8, which were suspected to be present in the vapor phase along with P_2 and P_4. A notable theoretical contribution came from Jones and Hohl[2] who systematically explored clusters up to P_8 with a simulated annealing technique based on the density functional method. Their most striking results are the prediction of a "cuneane" P_8 molecule as the most stable cluster besides tetrahedral P_4 and the prediction of a moderately stable P_6 cluster with C_{2v} symmetry formed by edge-on addition of P_2 to P_4.

There is no experimental evidence for species other than P_2 and P_4 in the vapor phase obtained from white phosphorus between 300 and 1470 K.[3a] Cationic clusters up to at least P_{24}^+ could be observed by mass spectroscopy in quenched vapor obtained from red phosphorus at 300K.[3b]

In this work we focus attention on even-membered larger phosphorus clusters up to P_{28}. Odd-membered clusters were not investigated, since our aim was to find phosphorus clusters and chain polymers which are energetically more stable than P_4, and radicals are unlikely candidates. Three major types of clusters will be considered: isolated polyhedral clusters, P_4 units linked by single bonds, and polyhedral units linked by two single bonds. From these investigations a consistent scheme of formation and structural features of red phosphorus emerges, which has some bearing on violet (Hittorf) phosphorus.[4] We further obtain hints for the possible existence of P_{12} and P_{16} clusters as new forms of phosphorus.

In our choice of potentially favorable structures we have been guided by chemical intuition and by a wealth of structures of substituted phosphanes[5] and polyphosphides.[6] However, some of those structural units do not lend themselves to medium-sized clusters. This includes the odd-membered subunits P_7 and P_9 which can only occur in larger aggregates unless dangling bonds are saturated.

II. Details of Computation

SCF and MP2 treatments as well as SCF force field calculations to compute vibrational frequencies have been carried out with the program system TURBOMOLE.[7] NMR shielding constants were computed by the SCF/GIAO method[8] with the program SHEILA,[7b] which uses a semidirect algorithm for the solution of coupled-perturbed Hartree–Fock (CPHF) equations for the magnetic field as perturbation.

(1) Corbridge, D. E. C. *The structural Chemistry of Phosphorus*; Elsevier Scientific Publishing Company: Amsterdam, 1974; p 13.
(2) Jones, R. O.; Hohl, D. *J. Chem. Phys.* **1990**, *92*, 6710 and references therein.
(3) (a) Bock, H.; Müller, H. *Inorg. Chem.* **1984**, *23*, 4365. (b) Martin, T. P. *Z. Phys.* **1986**, *D3*, 211.
(4) Thurn, M.; Krebs, M. *Acta Crystallogr.* **1969**, *B25*, 125.
(5) Baudler, M. *Angew. Chem.* **1987**, *99*, 429; *Angew. Chem., Int. Ed. Engl.* **1987**, *26*, 419.
(6) Schnering, H. G. v. *Angew. Chem.* **1981**, *93*, 44; *Angew. Chem., Int. Ed. Engl.* **1981**, *20*, 33.
(7) (a) Ahlrichs, R.; Bär, M.; Häser, M.; Horn, H.; Kölmel, C. *Chem. Phys. Lett.* **1989**, *162*, 162. (b) Häser, M.; Ahlrichs, R.; Baron, H. P.; Weis, P.; Horn, H. *Theoret. Chim. Acta* **1992**, *83*, 455.
(8) (a) Ditchfield, R. *Mol. Phys.* **1974**, *27*, 789. (b) Wolinski, K.; Hinton, J. F.; Pulay, P. *J. Am. Chem. Soc.* **1990**, *112*, 8251.

0002-7863/92/1514-9551$03.00/0 © 1992 American Chemical Society